

# Ternary Indides $RE\text{MgIn}$ ( $RE = \text{Y, La-Nd, Sm, Gd-Tm, Lu}$ ). Synthesis, Structure and Magnetic Properties

Rainer Kraft, Martin Valldor, Daniel Kurowski, Rolf-Dieter Hoffmann, and Rainer Pöttgen

Institut für Anorganische und Analytische Chemie, Westfälische Wilhelms-Universität Münster,  
Wilhelm-Klemm-Straße 8, D-48149 Münster (Germany)

Reprint requests to R. Pöttgen. E-mail: pottgen@uni-muenster.de

Z. Naturforsch. **59b**, 513–518 (2004); received Februar 25, 2004

The equiatomic rare earth-magnesium-indium compounds  $RE\text{MgIn}$  ( $RE = \text{Y, La-Nd, Sm, Gd-Tm, Lu}$ ) were prepared from the elements in sealed tantalum tubes inside a water-cooled sample chamber of an induction furnace. All compounds were characterized through their X-ray powder patterns. They crystallize with the hexagonal  $\text{ZrNiAl}$  type structure, space group  $P6_2/m$ , with three formula units per cell. The structure of  $\text{SmMgIn}$  was refined from X-ray single crystal diffractometer data:  $a = 761.3(2)$ ,  $c = 470.3(1)$  pm,  $wR2 = 0.0429$ , 380  $F^2$  values and 14 variable parameters. The  $\text{DyMgIn}$ ,  $\text{HoMgIn}$ , and  $\text{TmMgIn}$  structures have been analyzed using the Rietveld technique. The  $RE\text{MgIn}$  structures contain two crystallographically independent indium sites, both with tri-capped trigonal prismatic coordination:  $\text{In1Sm}_6\text{Mg}_3$  and  $\text{In2Mg}_6\text{Sm}_3$ . Together the magnesium and indium atoms form a three-dimensional  $[\text{MgIn}]$  network with  $\text{Mg-Mg}$  distances of 320 and  $\text{Mg-In}$  distances in the range 294–299 pm. Temperature dependent magnetic susceptibility data show Curie-Weiss behavior for  $\text{DyMgIn}$ ,  $\text{HoMgIn}$ , and  $\text{TmMgIn}$  with experimental magnetic moments of 11.0(1)  $\mu_B/\text{Dy}$  atom, 10.9(1)  $\mu_B/\text{Ho}$  atom, and 7.5(1)  $\mu_B/\text{Tm}$  atom. The three compounds order antiferromagnetically at  $T_N = 22(2)$  K ( $\text{DyMgIn}$ ), 12(1) K ( $\text{HoMgIn}$ ), and 3(1) K ( $\text{TmMgIn}$ ).

**Key words:** Rare Earth Compounds, Crystal Chemistry, Magnetochemistry

## Introduction

The equiatomic intermetallics  $RTX$  ( $R =$  alkaline earth or rare earth element;  $T =$  late transition element;  $X =$  main group element) have attracted considerable interest in recent years due to their peculiar magnetic and electrical properties [1]. These compounds show a large structural variety. So far, 30 different structure types [2,3] have been observed for these intermetallics. In the Pearson Handbook [4] and in the crystal chemical data bases, it is possible to find more than 1500 representatives which crystallize with the simple  $RTX$  composition.

In addition to the large number of  $RTX$  intermetallics, only little information is available on related or even isotypic  $RXX'$  compounds, where the transition metal is fully substituted by another main group element. Such a substitution has a large influence on the electronic situation of the rare earth element, and thus on the magnetic and electrical properties. So far, most investigations were performed on  $RE\text{AlSi}$  and  $RE\text{AlGe}$  compounds ( $RE =$  rare earth element) [4–6].

We have recently started a more systematic study of the systems  $RE\text{MgGa}$  [7,8]. These compounds crys-

tallize with the hexagonal  $\text{ZrNiAl}$  [9–11] type structure with a complete ordering of the magnesium and gallium atoms. Magnetic susceptibility measurements revealed antiferromagnetic ordering at  $T_N = 3.1$  K for  $\text{CeMgGa}$  [7], with a metamagnetic transition at a critical field of 1.0 T.  $\text{GdMgGa}$  [12] has a stable antiferromagnetic ( $T_N = 15.3$  K) ground state up to an external field of 9 T. In contrast,  $\text{GdMgIn}$  with the same crystal structure [12] shows no evidence for magnetic ordering down to 4 K.

Herein we report on the synthesis and structural investigation of the remaining compounds in the  $RE\text{MgIn}$  series. Additionally, we present the magnetic properties of  $\text{DyMgIn}$ ,  $\text{HoMgIn}$ , and  $\text{TmMgIn}$ .

## Experimental Section

### Synthesis

Starting materials for the preparation of the  $RE\text{MgIn}$  samples were ingots of the rare earth metals (Johnson Matthey, Chempur or Kelpin, > 99.9%), a magnesium rod (Johnson Matthey,  $\varnothing$  16 mm, > 99.5%), and indium tear drops (Johnson Matthey, > 99.9%). With the exception of thulium, which has a relatively high vapor pressure, all rare earth

Table 1. Lattice parameters of the hexagonal indides REMgIn, (space group  $P6_2m$ , ZrNiAl type).

Compound	<i>a</i> (pm)	<i>c</i> (pm)	<i>V</i> (nm <sup>3</sup> )
YMgIn	748.9(2)	464.45(9)	0.2256
LaMgIn	782.6(2)	481.08(9)	0.2552
CeMgIn	774.9(3)	477.7(2)	0.2484
PrMgIn	771.5(3)	475.0(1)	0.2448
NdMgIn	768.0(3)	473.8(2)	0.2420
SmMgIn	761.3(2)	470.3(1)	0.2361
GdMgIn	755.3(1)	467.99(8)	0.2312
TbMgIn	752.0(3)	466.3(2)	0.2284
DyMgIn	749.2(1)	464.58(7)	0.2258
HoMgIn	746.7(2)	463.76(8)	0.2239
ErMgIn	744.3(1)	462.74(6)	0.2220
TmMgIn	742.4(2)	461.4(1)	0.2202
LuMgIn	739.0(1)	460.20(6)	0.2177

Table 2. Crystal data and structure refinement for SmMgIn (space group  $P6_2m$ ; *Z* = 3).

Empirical formula	SmMgIn
Molar mass	289.48 g/mol
Unit cell dimensions	Table 1
Calculated density	6.11 g/cm <sup>3</sup>
Crystal size	5 × 15 × 20 μm <sup>3</sup>
Transm. ratio (max/min)	0.612 / 0.438
Absorption coefficient	25.7 mm <sup>-1</sup>
<i>F</i> (000)	369
Detector distance	60 mm
Exposure time	50 min
$\omega$ Range; increment	0° – 180°, 1°
Integr. parameters <i>A</i> , <i>B</i> , <i>EMS</i>	14.0, 4.0, 0.012
$\theta$ Range	3° to 34°
Range in <i>hkl</i>	±11, −9 ≤ <i>k</i> ≤ 11, ±7
Total no. reflections	2895
Independent reflections	380 ( <i>R</i> <sub>int</sub> = 0.1012)
Reflections with <i>I</i> > 2σ( <i>I</i> )	363 ( <i>R</i> <sub>sigma</sub> = 0.0477)
Data/parameters	380 / 14
Goodness-of-fit on <i>F</i> <sup>2</sup>	1.332
Final <i>R</i> indices [ <i>I</i> > 2σ( <i>I</i> )]	<i>R</i> 1 = 0.0346, <i>wR</i> 2 = 0.0426
<i>R</i> Indices (all data)	<i>R</i> 1 = 0.0383, <i>wR</i> 2 = 0.0429
Extinction coefficient	0.0012(4)
Flack parameter	−0.03(4)
Largest diff. peak and hole	1.70 and −1.72 e/Å <sup>3</sup>

metal pieces were first melted under argon to small buttons in an arc-melting furnace [13]. The argon was purified over titanium sponge (900 K), silica gel, and molecular sieves. Pieces of the magnesium rod (the surface of the rod was first cut on a turning lathe in order to remove surface impurities), the arc-melted rare earth metal buttons, and pieces of the indium tear drops were then weighed in the ideal 1:1:1 atomic ratios and sealed in tantalum ampoules under an argon pressure of about 800 mbar. The tantalum tubes were placed in a water-cooled sample chamber [14] of an induction furnace (Hüttinger Elektronik, Freiburg, Typ TIG 1.5/300). In order to get a homogeneous melt, the mixtures of the elements were first heated under flowing argon for 30 s with *ca.* 70% of the maximum power output. The reaction between

Table 3. Atomic coordinates and isotropic displacement parameters (pm<sup>2</sup> for *U*<sub>eq</sub> and Å<sup>2</sup> for *B*) for SmMgIn, DyMgIn, HoMgIn and TmMgIn (space group  $P6_2m$ ). *U*<sub>eq</sub> is defined as a third of the trace of the orthogonalized *U*<sub>ij</sub> tensor. The standard deviations for the X-ray powder data are already multiplied with the Bérar-Lelann factor.

Atom	Wyckoff site	<i>x</i>	<i>y</i>	<i>z</i>	<i>U</i> <sub>eq</sub> / <i>B</i>
<i>SmMgIn</i> (single crystal data)					
Sm	3 <i>f</i>	0.56823(10)	0	0	104(1)
Mg	3 <i>g</i>	0.2428(6)	0	1/2	133(10)
In1	2 <i>d</i>	1/3	2/3	1/2	95(2)
In2	1 <i>a</i>	0	0	0	126(3)
<i>DyMgIn</i> (powder data)					
Dy	3 <i>f</i>	0.5659(3)	0	0	0.32(8)
Mg	3 <i>g</i>	0.243(2)	0	1/2	0.8(4)
In1	2 <i>d</i>	1/3	2/3	1/2	0.9(1)
In2	1 <i>a</i>	0	0	0	1.5(2)
<i>HoMgIn</i> (powder data)					
Ho	3 <i>f</i>	0.5662(4)	0	0	1.38(9)
Mg	3 <i>g</i>	0.241(2)	0	1/2	0.6(4)
In1	2 <i>d</i>	1/3	2/3	1/2	0.4(9)
In2	1 <i>a</i>	0	0	0	0.36(13)
<i>TmMgIn</i> (powder data)					
Tm	3 <i>f</i>	0.5642(4)	0	0	0.69(7)
Mg	3 <i>g</i>	0.241(3)	0	1/2	1.3(4)
In1	2 <i>d</i>	1/3	2/3	1/2	0.39(10)
In2	1 <i>a</i>	0	0	0	1.02(15)

Table 4. Interatomic distances (pm), calculated from single crystal data using the lattice parameters taken from X-ray powder data of SmMgIn.

Sm:	4	In1	326.0(1)	Mg:	2	In1	294.3(3)
	1	In2	328.7(1)		2	In2	299.1(3)
	2	Mg	341.6(4)		2	Mg	320.2(8)
	4	Mg	369.8(1)		2	Sm	341.6(4)
	4	Sm	391.1(1)		4	Sm	369.8(1)
In1:	3	Mg	294.3(3)	In2:	6	Mg	299.1(3)
	6	Sm	326.0(1)		3	Sm	328.7(1)

the elements was visible through a slight heat flash. Subsequently the tubes were annealed at *ca.* 800 K for another 4 h and finally quenched by switching off the power supply.

All REMgIn samples could be broken mechanically off the ampoule walls. No reactions with the crucible material was detected. Compact pieces and powders of the REMgIn compounds are stable in air over long periods of time. Powders are dark grey and the single crystals exhibit metallic lustre.

#### X-ray film data and structure refinement of SmMgIn

All samples were characterized through their Guinier powder patterns using Cu-K<sub>α1</sub> radiation and α-quartz (*a* = 491.30, *c* = 540.46 pm) as an internal standard. The Guinier camera was equipped with an imaging plate system (Fujifilm BAS-1800). The lattice parameters (Table 1) were obtained from least-squares fits of the Guinier data. To ensure cor-

Empirical formula	DyMgIn	HoMgIn	TmMgIn
Formula weight (g/mol)	301.62	304.05	308.06
Lattice parameters (diffractometer data)	$a = 749.92$ pm $c = 465.11$ pm $V = 0.2265$ nm <sup>3</sup>	$a = 747.55$ pm $c = 464.37$ pm $V = 0.2247$ nm <sup>3</sup>	$a = 743.31$ pm $c = 462.18$ pm $V = 0.2211$ nm <sup>3</sup>
Calculated density (g/cm <sup>3</sup> )	6.63	6.74	6.94
Absorption correction ( $\mu$ R)	1.40	1.40	1.40
$F(000)$	381	384	390
Range in $2\theta$	10–100	10–100	5–100
Scan mode, step width	$\omega/2\theta$ , 0.02	$\omega/2\theta$ , 0.02	$\omega/2\theta$ , 0.02
Preferred orientation	101 / 0.954(4)	111 / 0.955(4)	111 / 0.951(3)
No. data points	4500	4500	4750
Total no. Bragg reflections	75	74	72
Asymmetry parameters	0.044(8) 0.0297(12)	0.051(7) 0.0250(11)	–0.004(4) 0.0245(10)
No. structure parameters	8	8	8
No. total parameters	17	17	17
$R_F$ , $R_{wp}$	0.056, 0.133	0.058, 0.135	0.036, 0.110
$R_{Bragg(I)}$ , goodness-of-fit, ( $\chi^2$ )	0.065, 1.50, 1.64	0.070, 1.92, 2.07	0.054, 3.88, 4.13
Bérar-Lelann Factor	1.92	2.36	3.19

Table 5. X-ray powder data and structure refinement for DyMgIn, HoMgIn and TmMgIn (hexagonal,  $P6_2m$ ,  $Z = 3$ ).

rect indexing, the observed patterns were compared to calculated ones [15] using the atomic positions obtained from the structure refinements. The lattice parameters derived for the powders and the single crystals agreed well. For GdMgIn our lattice parameters show good agreement with the data from Canepa *et al.* of  $a = 755.0(2)$  and  $c = 467.8(1)$  pm [12].

Irregularly shaped single crystals of SmMgIn were isolated from the annealed samples by mechanical fragmentation and subsequently examined by Laue photographs on a Buerger precession camera (equipped with an imaging plate system Fujifilm BAS–1800) in order to establish suitability for intensity data collection. Intensity data were recorded at room temperature by use of a Stoe IPDS–II diffractometer with graphite monochromatized Mo- $K_{\alpha}$  radiation. The absorption correction for this crystal was numerical. All relevant crystallographic data for the data collection and evaluation are listed in Table 2.

The isotypy of SmMgIn with the previously reported gallium compounds REMgGa [7, 8] was already evident from the X-ray powder data. The atomic positions of SmMgGa [8] were taken as starting values and the structure was refined using SHELXL-97 (full-matrix least-squares on  $F_o^2$ ) [16] with anisotropic atomic displacement parameters for all sites.

As a check for a possible Mg/In mixing, the occupancy parameters of the magnesium and indium positions were refined in a separate series of least-squares cycles. The three sites are fully occupied within two standard deviations. In the last cycles, the ideal occupancies were assumed again. Refinement of the correct absolute structure was ensured through refinement of the Flack parameter [17, 18]. A final difference Fourier synthesis revealed no significant residual peaks (see Table 2). The positional parameters and interatomic distances are listed in Tables 3 and 4. Listings of the

observed and calculated structure factors are available.\* The SmMgIn single crystal measured on the diffractometer has been analyzed by EDX using a Leica 420 I scanning electron microscope with SmF<sub>3</sub>, MgO, and InAs as standards. No impurity elements were detected.

#### Rietveld data of DyMgIn, HoMgIn, and TmMgIn

The growth of suitable crystals for an X-ray study of the indium compounds was not as successful as for the isotypic gallium compounds [7, 8]. We have therefore investigated some of the REMgIn compounds on a powder diffractometer (Stoe Stadi P, Cu- $K_{\alpha 1}$  radiation) in order to perform full profile Rietveld refinements. The data for DyMgIn, HoMgIn, and TmMgIn are presented in Fig. 1. The measurements were performed in Debye-Scherrer geometry using Cu- $K_{\alpha 1}$  radiation ( $\lambda = 154.0598$  pm, Ge monochromator). All experimental details are listed in Table 5.

The Rietveld calculations were performed with the Fullprof [19] software. The background was set manually and the profiles were modelled using the pseudo-Voigt function. The limit of peak asymmetry was set to 60 degrees ( $2\theta$ ) and an arbitrary absorption value of  $\mu R = 1.4$  has been used. The experimental data of the three refinements are summarized in Table 5. The standard deviations of the refined parameters have been multiplied with the Bérar-Lelann factor [20]. The resulting positional parameters are listed in Table 3. The standard deviations of the x parameters for the rare earth metal and magnesium position are about 3 times larger for the X-ray powder data as compared to the single crystal data of SmMgIn. Nevertheless, the powder data fully confirm the struc-

\*Details may be obtained from: Fachinformationszentrum Karlsruhe, D-76344 Eggenstein-Leopoldshafen (Germany), by quoting the Registry No. CSD–413808.

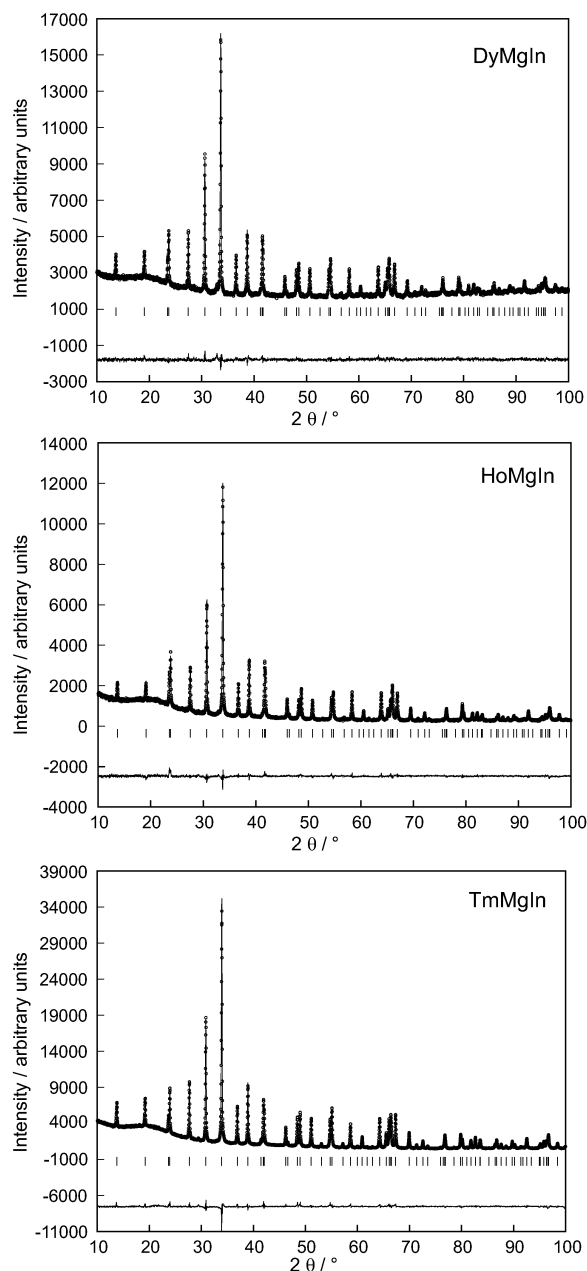


Fig. 1. Rietveld refinement plots for DyMgIn, HoMgIn, and TmMgIn, in which the observed intensities are indicated with open circles and the calculated pattern with a line on top of the circles. The vertical lines indicate the Bragg positions. The difference  $y(\text{obs})-y(\text{calc})$  is drawn below the Bragg indicators.

ture of these compounds and we could show that these three samples are very pure on the level of X-ray powder diffraction.

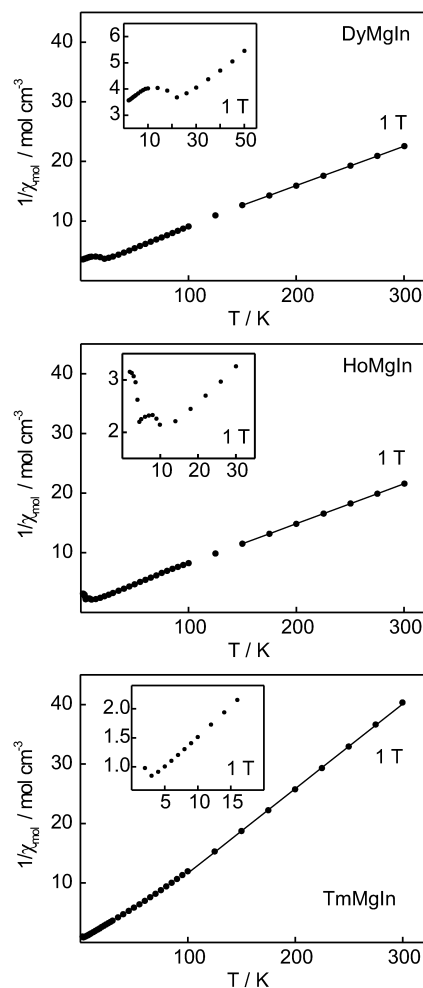


Fig. 2. Temperature dependence of the reciprocal magnetic susceptibilities of DyMgIn, HoMgIn, and TmMgIn, measured at external fields of 1 T. The behaviour at low temperatures is presented in the inserts. The straight line corresponds to the Curie-Weiss fit.

#### Magnetic data of DyMgIn, HoMgIn, and TmMgIn

The magnetic susceptibilities of polycrystalline, powdered samples of DyMgIn, HoMgIn, and TmMgIn were determined with a Quantum Design SQUID magnetometer and a PPMS in the temperature range 2 to 300 K with magnetic flux densities up to 9 T. The samples were enclosed in small gelatin capsules and fixed at the sample holder rod. The samples were then cooled to 2 K in zero magnetic field and slowly heated to room temperature in the applied external field.

The temperature dependencies of the reciprocal magnetic susceptibilities are presented in Fig. 2. The three compounds show Curie-Weiss behavior above 100 K with experimen-

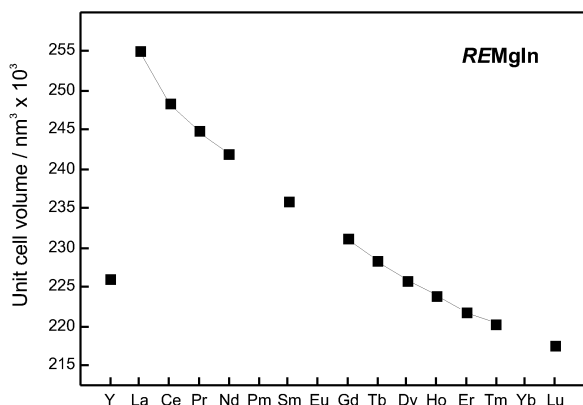


Fig. 3. Plot of the cell volumes of the hexagonal REMgIn compounds.

tal magnetic moments of 11.0(1)  $\mu_B$ /Dy atom (DyMgIn), 10.9(1)  $\mu_B$ /Ho atom (HoMgIn), and 7.5(1)  $\mu_B$ /Tm atom (TmMgIn), close to the free ion values [21] of 10.65  $\mu_B$ , 10.61  $\mu_B$ , and 7.56  $\mu_B$  for  $Dy^{3+}$ ,  $Ho^{3+}$ , and  $Tm^{3+}$ , respectively. The three compounds order antiferromagnetically at  $T_N = 22(1)$  K (DyMgIn), 12(1) K (HoMgIn), and 3(1) K (TmMgIn). A second minimum in the reciprocal susceptibility of HoMgIn most likely indicates a spin reorientation. The paramagnetic Curie temperatures (Weiss constants) are  $\Theta = -42(2)$  K (DyMgIn),  $-22(2)$  K (HoMgIn), and  $+19(1)$  K (TmMgIn).

More detailed magnetization measurements and neutron diffraction experiments [22] are currently in progress in order to establish the magnetic structures of these compounds.

## Discussion

Twelve new rare earth–magnesium–indium compounds have been synthesized and structurally characterized. The cell volumes of the REMgIn compounds decrease from the lanthanum to the lutetium compound as expected from the lanthanoid contraction (Fig. 3). CeMgIn smoothly fits in the curve, indicating trivalent cerium. The cell volume of YMgIn fits between those of TbMgIn and DyMgIn, similar to the series of REMgGa compounds [8].

The crystal chemistry of the REMgIn series is more or less similar to the REMgGa series. For drawings of the relatively simple crystal structure we refer to our previous manuscript [8]. Due to the much larger atomic radius of indium (163 pm) as compared to gallium (122 pm) [23], the REMgIn compounds have significantly larger cell parameters. Thus, we also observe an increase of all interatomic distances in the structure of SmMgIn as compared to SmMgGa [8]. Within the three-dimensional [MgIn] network, the Mg–In distances range from 294 to 299 pm, slightly longer than the sum of the covalent radii of 286 pm [23]. The Mg–Mg distances within the trigonal prisms around the origin of the cell are 320 pm, similar to the average Mg–Mg distance in *hcp* magnesium [24]. We can thus assume relatively strong Mg–In and Mg–Mg interactions within the [MgIn] network.

The structure refinements gave no hint for mixing of the magnesium and indium atoms in contrast to transition metal–magnesium–indium intermetallics. The binary compounds  $Mg_3Ir$ ,  $IrIn_2$ , and  $IrIn_3$  show pronounced solid solutions  $Mg_{3-x}In_xIr$ ,  $IrIn_{2-x}Mg_x$ , and  $IrIn_{3-x}Mg_x$ , where all magnesium (indium) sites show mixed Mg/In occupancies [25, 26].

With europium or ytterbium as rare earth metal component no isotypic REMgIn compound was observed. A solid solution  $EuMg_{1-x}In_{1+x}$  with the hexagonal  $MgNi_2$  structure was observed with europium, while an unknown structure with a homogeneity range is formed with ytterbium. Detailed studies of these solid solutions are in progress.

## Acknowledgments

We thank Dipl.-Ing. U. Ch. Rodewald for the collection of the single crystal data and H.-J. Göcke for the work at the scanning electron microscope. This work was financially supported by the Deutsche Forschungsgemeinschaft.

- [1] A. Szytuła, J. Leciejewicz, Handbook of Crystal Structures and Magnetic Properties of Rare Earth Intermetallics, CRC Press, Boca Raton, Florida (1994).
- [2] M. L. Fornasini, F. Merlo, J. Alloys Compd. **219**, 63 (1995).
- [3] R.-D. Hoffmann, R. Pöttgen, Z. Kristallogr. **216**, 127 (2001).

- [4] P. Villars, L. D. Calvert, Pearson's Handbook of Crystallographic Data for Intermetallic Phases, Second Edition, American Society for Metals, Materials Park, OH 44073 (1991).
- [5] R. Pöttgen, D. Johrendt, Chem. Mater. **12**, 875 (2000).
- [6] R. Pöttgen, D. Johrendt, D. Kußmann, Structure Property Relations of Ternary Equiatomic YbTX Inter-

- metallics, in K.A. Gschneidner (Jr.) and L. Eyring (eds), Handbook on the Chemistry and Physics of Rare Earths, vol. 32, chapter 207 (2001).
- [7] R. Kraft, D. Kaczorowski, R. Pöttgen, *Chem. Mater.* **15**, 2998 (2003).
- [8] R. Kraft, M. Valldor, R. Pöttgen, *Z. Naturforsch.* **58b**, 827 (2003).
- [9] M. F. Zumdick, R.-D. Hoffmann, R. Pöttgen, *Z. Naturforsch.* **54b**, 45 (1999).
- [10] A. E. Dwight, M. H. Mueller, R. A. Conner (Jr.), J. W. Downey, H. Knott, *Trans. Met. Soc. AIME* **242**, 2075 (1968).
- [11] P. I. Kropyakevich, V. Ya. Markiv, E. V. Melnyk, *Dopov. Akad. Nauk. Ukr. RSR, Ser. A*, 750 (1967).
- [12] F. Canepa, M. L. Fornasini, F. Merlo, M. Napoletano, M. Pani, *J. Alloys Compd.* **312**, 12 (2000).
- [13] R. Pöttgen, Th. Gulden, A. Simon, *GIT Labor Fachzeitschrift* **43**, 133 (1999).
- [14] D. Kußmann, R.-D. Hoffmann, R. Pöttgen, *Z. Anorg. Allg. Chem.* **624**, 1727 (1998).
- [15] K. Yvon, W. Jeitschko, E. Parthé, *J. Appl. Crystallogr.* **10**, 73 (1977).
- [16] G. M. Sheldrick, SHELXL-97, Program for Crystal Structure Refinement, University of Göttingen, Germany (1997).
- [17] H. D. Flack, G. Bernadinelli, *Acta Crystallogr. A* **55**, 908 (1999).
- [18] H. D. Flack, G. Bernadinelli, *J. Appl. Crystallogr.* **33**, 1143 (2000).
- [19] T. Roisnel, J. Rodríguez-Carvajal, Fullprof.2k V. 2.0 (2001) Laboratoire Lon Brillouin (CEA-CNRS), 91191 Gif-sur-Yvette Cedex (France).
- [20] J.-F. Béar, P. Lelann, *J. Appl. Crystallogr.* **24**, 1 (1991).
- [21] H. Lueken, *Magnetochemie*, Teubner, Stuttgart (1999).
- [22] W. Kockelmann, D. Kurowski, R. Kraft, R. Pöttgen, unpublished results.
- [23] J. Emsley, *The Elements*, Oxford University Press, Oxford (1999).
- [24] J. Donohue, *The Structures of the Elements*, Wiley, New York (1974).
- [25] V. Hlukhyy, R.-D. Hoffmann, R. Pöttgen, *Z. Anorg. Allg. Chem.* **630**, 68 (2004).
- [26] V. Hlukhyy, R.-D. Hoffmann, R. Pöttgen, *Intermetallics*, in press.